

HIGH-PERFORMANCE CONTROL OF A PZT SCANNER

B. Bhikkaji,¹ M. Ratnam,
A. J. Fleming and S. O. R. Moheimani.

*Dept of Electrical Engineering and Computer Science, The
University of Newcastle, NSW, Australia*

Abstract:

A piezoelectric tube of the type typically used for actuation in Scanning Tunneling Microscopes (STMs) and Atomic Force Microscopes (AFMs) is considered. Actuation of this piezoelectric tube is hampered by the presence of a lightly damped low frequency resonant mode. This resonant mode is first identified and then damped using a Positive Velocity and Position Feedback (PVPF) controller, a control technique which is proposed in this paper. Inputs are then shaped such that the closed loop system tracks a raster pattern.

Keywords:

Piezoelectric tubes, System Identification, Resonance, Damping, Feedback Control and Input Shaping.

1. INTRODUCTION

Scanning Tunneling Microscopes (STM) and Atomic Force Microscopes (AFM) are used at extreme magnifications for profiling material surfaces at micro to atomic resolution.

In general the scanning unit of the STMs and AFMs would contain a probe the tip of which is placed in close proximity (typically few Angstroms) to the surface of the material sample. Scanning the material surface is done by actuating either the probe or the material sample in a raster pattern. Many STMs and AFMs use piezoelectric tubes (commercially known as PZT scanners) for actuation. In such STMs and AFMS either the probe or the seat of the material sample is attached to the piezoelectric tube, and scanning is done by actuating the piezoelectric tube in a raster pattern.

One of the advantages of using piezoelectric tubes for scanning is that under certain experimental conditions their dynamics can be well approximated by linear models, see (G. Schitter and A. Stemmer, 2004; N. Tamer and M. Daleh, 1994). However, the linear models normally possess lightly damped resonant modes, which make the piezoelectric tubes susceptible to mechanical vibrations. Furthermore non-linearities such as creep and hysteresis have to be taken into account when actuating the tube with low frequency inputs (near DC signals) and high amplitude inputs respectively (K. K. Leang and S. Devasia, 2002). The presence of mechanical vibrations and the non-linearities hinder the actuation of the tube.

Positive Velocity and Position Feedback (PVPF) control is a controller design technique introduced in this paper to damp the unwanted vibrations of the piezoelectric tube. As the name suggests the inputs to this feedback controller are position and velocity of the system output, (*i.e.* the inputs are y and \dot{y} , if y is the system output), and the

¹ Corresponding author, *email:*
Bharath.Bhikkaji@newcastle.edu.au, *Phone:* +61 2
49217223

controller output is positively feedback into the system. In the recent past Caughey and co-authors had introduced a control technique known as the Positive Position Feedback (PPF) control, (J. L. Fanon and T. K. Caughey, 1990), to suppress the mechanical vibrations in a structure. The model structures of both PPF and PVPF bare some similarities. In fact PVPF can be thought of as a modification of the PPF that is technically more suited for the piezoelectric tube.

Nonlinearity in the form of hysteresis appears when a piezoelectric tube is actuated using high amplitude signals driven by voltage sources. Since the late 1980's, it has been known that actuating piezoelectric transducers with current or charge sources rather than voltage sources significantly reduces hysteresis (Newcomb and Flinn, 1982). In fact it has been noted that using current or charge sources, a five-fold reduction in hysteresis can be achieved (Ge and Jouaneh, 1996). In (A. J. Fleming and S. O. R. Moheimani, Feb 2003), the authors have designed a charge source for the general purpose of exciting piezoelectric actuators without encountering hysteresis. In this work, this charge source is used for actuating the piezoelectric tube in order to avoid hysteresis.

In this paper a piezoelectric tube of the type typically used in the scanning unit of the STMs and AFMs is considered, see Figure 1. In Section 2 linear models are constructed for the tube and the resonant mode of interest is identified. The need for designing a feedback controller is motivated in Section 3. The concept of PVPF is introduced and a PVPF controller is designed to damp the resonant mode in Sections 4 and 5 respectively. Inputs are also designed in Section 5 for accurate actuation of the closed loop system in a raster pattern, as shown in Figure 2.

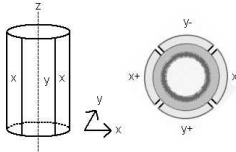


Fig. 1. Illustration of a quartered piezoelectric tube with its dimensions exaggerated

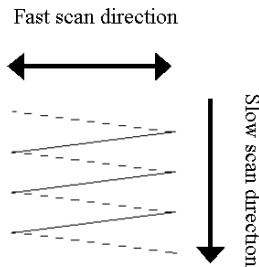


Fig. 2. Illustration of the raster pattern.

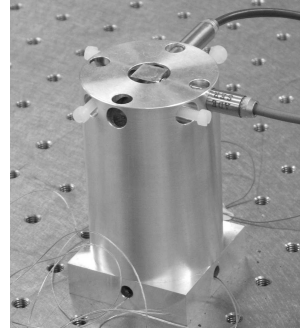


Fig. 3. The piezoelectric tube mounted inside an aluminum enclosure. The capacitive sensors are shown secured at right angles to the perpendicular faces of the cube mounted onto the tube tip.

2. SYSTEM IDENTIFICATION

In this section the piezoelectric tube is modeled as a linear system.

2.1 Experimental Setup

The piezoelectric tube considered here is a symmetric thin walled cylindrical tube made of a piezoelectric material, with its inner and the outer walls finely coated with a layer of copper. The copper coating on the inner and outer walls of the tube act as electrodes. The outer electrode is axially quartered into four equal sections. A pair of the opposite sections of the quartered electrode is referred to as the $x-x$ electrodes and the other pair is referred as the $y-y$ electrodes, see Figure 1. A jig is constructed to hold the piezoelectric tube along the z axis. A small aluminum cube is bonded to the upper end of the tube. This cube represents the seat where the materials that need to be scanned are placed. The heads of two ADE Technologies 4810 capacitive sensors are placed in close proximity to the adjacent faces of the aluminum cube in the x and y directions respectively. The inner electrode of the piezoelectric tube is grounded. One electrode each of the $x-x$ and $y-y$ pairs, referred to as x^+ and y^+ respectively, are chosen as the input ends of the piezoelectric tube, and the corresponding opposite ends, referred to as x^- and y^- respectively, are chosen as the output ends of the piezoelectric tube. The whole setup, consisting of the piezoelectric tube with the bonded aluminum cube and the heads of the capacitive sensors, is placed in a specially constructed circular enclosure, illustrated in Figure 3. The circular enclosure protects the experimental setup from external disturbances.

When charge signals Q_{x^+} and Q_{y^+} are applied at the electrodes x^+ and y^+ respectively, the piezoelectric tube deforms inducing voltages V_{x^-} and V_{y^-} at the output electrodes x^- and y^- ,

respectively. The induced voltages $[V_{x^-}, V_{y^-}]^\top$ are recorded and taken as outputs of the system. Furthermore, due to the deformation of the tube, the capacitance between the aluminum cube and the head of the capacitive sensors change. The change in the capacitance is measured by capacitive sensor in terms of the distance between its head and the aluminum cube. This distance, denoted by $C = [C_x, C_y]^\top$, is also recorded as an output. The outputs C_x and C_y indicate the lateral displacements of the tube in the x and y directions respectively.

Quantitatively the piezoelectric tube setup is modeled as having linear subsystems V and C of the form

$$Y_v(s) \triangleq G_{vq}(s)U(s) \quad (1)$$

and

$$Y_c(s) \triangleq G_{cq}(s)U(s) \quad (2)$$

respectively, where $U(s)$ is the Laplace transform of the input signal $[Q_{x^+}, Q_{y^+}]^\top$, $Y_v(s)$ and $Y_c(s)$ are the Laplace transforms of the voltages $[V_{x^-}, V_{y^-}]$ and capacitive sensor outputs $[C_x, C_y]^\top$, respectively, and

$$G_{vq}(s) = \begin{bmatrix} G_{xx}(s) & G_{xy}(s) \\ G_{yx}(s) & G_{yy}(s) \end{bmatrix} \quad (3)$$

and

$$G_{cq}(s) = \begin{bmatrix} G_{xc_x}(s) & G_{xc_y}(s) \\ G_{yc_x}(s) & G_{yc_y}(s) \end{bmatrix} \quad (4)$$

are a 2×2 transfer function matrices.

2.2 Modelling

An experiment is performed on the piezoelectric tube by inputting swept sine waves into the electrodes x^+ and y^+ , and recording the corresponding voltage outputs at x^- and y^- and the capacitive sensor outputs C_x and C_y . Using a HP 35670A dual channel Spectrum Analyser, the recorded input output data is processed to obtain Frequency response functions (FRF) $G_{vq}(i\omega)$ and $G_{cq}(i\omega)$ corresponding to the transfer functions $G_{vq}(s)$ and $G_{cq}(s)$, respectively, in the non-parametric form.

In Figures 4 and 5 the magnitude and the phase of the FRFs $G_{xx}(i\omega)$, $G_{yy}(i\omega)$, $G_{xy}(i\omega)$ and $G_{yx}(i\omega)$, obtained from the Spectrum Analyser, are plotted. Similarly, in Figures 6 and 7 the magnitude and the phase of the FRFs $G_{xc_x}(i\omega)$, $G_{xc_y}(i\omega)$, $G_{yc_x}(i\omega)$ and $G_{yc_y}(i\omega)$ are plotted. It is worth noting that the cross coupling terms $G_{xc_y}(i\omega)$ and

$G_{yc_x}(i\omega)$ in the subsystem C are negligible in magnitude, except at the frequencies around the resonance, when compared with the direct terms $G_{xc_x}(i\omega)$ and $G_{yc_y}(i\omega)$. In other words, input Q_{x^+} will have little effect on the capacitive sensor output C_y in the y direction, unless the frequencies close to the resonance are excited. The same holds for input Q_{y^+} and the capacitive sensor output C_x .

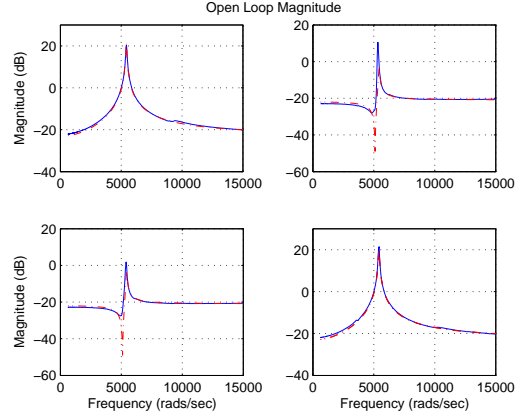


Fig. 4. Bode magnitude plots of the non-parametric models (solid) along with their corresponding parametric models (dashed dots).

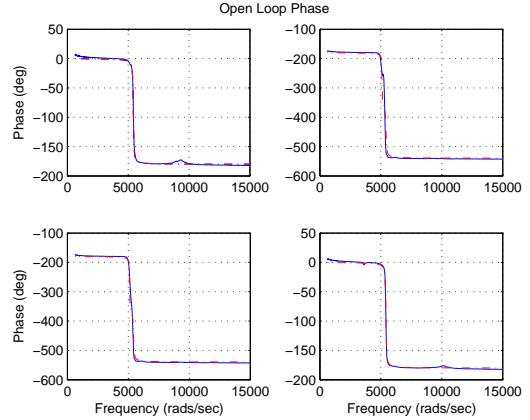


Fig. 5. Bode phase plots of the non-parametric models (solid) along with their corresponding parametric models (dashed dots).

Since there is only one resonance frequency in the FRFs $G_{xx}(i\omega)$, $G_{yy}(i\omega)$, $G_{xc_x}(i\omega)$ and $G_{yc_y}(i\omega)$, in the frequency regions presented in the plots, second order models are fitted to their corresponding non-parametric data. The following models were found to fit the non-parametric data:

$$G_{xx}(s) = G_{yy}(s) = \frac{k_1}{s^2 + 2\sigma\omega s + \omega^2} + d_1, \quad (5)$$

$$G_{xc_x}(s) = G_{yc_y}(s) = \frac{c_1 s^2 + c_2 s + c_3}{s^2 + 2\sigma\omega s + \omega^2}, \quad (6)$$

3. FEED-FORWARD CONTROL

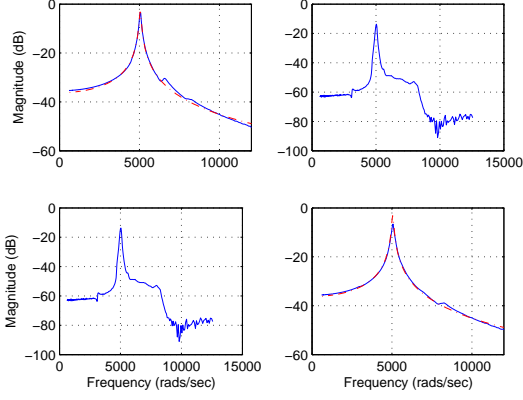


Fig. 6. Bode plots of the non-parametric models (solid) along with their corresponding parametric models (dashed dots).

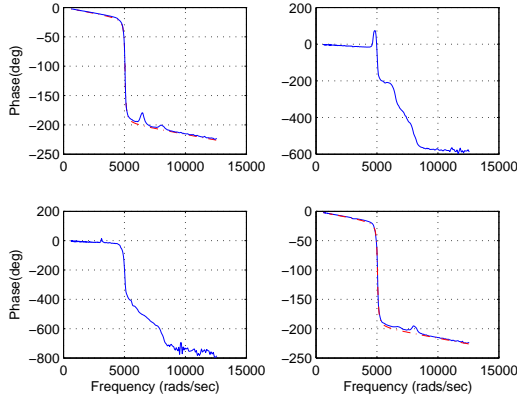


Fig. 7. Bode plots of the non-parametric models (solid) along with their corresponding parametric models (dashed dots).

where the model parameters are as tabulated in Table 1. In Figures 4 and 5 magnitude and phase

k_1	4.8736×10^6
$2\sigma\omega$	78.9826
ω^2	2.942×10^7
d_1	-7.8×10^{-2}
c_1	0.0015
c_2	0.1185
c_3	5.874×10^5

Table 1. Parameter values of the FRFs $G_{xx}(s)$, $G_{yy}(s)$, $G_{c_{xx}}(s)$ and $G_{c_{yy}}(s)$.

of the parametric fit (5) are plotted along with the non-parametric data, and in Figures 6 and 7 magnitude and phase of the parametric fit (6) are plotted along with the corresponding non-parametric data. Parametric fits for cross coupling terms $G_{xy}(s)$, $G_{yx}(s)$, $G_{xc_y}(s)$ and $G_{yc_x}(s)$ are not presented here as they are not used for actuating the tube.

As mentioned earlier the goal is to actuate the piezoelectric tube in a raster pattern. Therefore a desired trajectory for the piezoelectric tube would be to repeatedly trace straight lines back and forth in x direction, while slowly increasing its position in the y direction, as illustrated in Figure 2. A common practice to achieve such a path is to input a triangular waveform in x^+ electrode and a “very slowly” increasing ramp in the y^+ electrode as reference signals for the system. Normally for illustration purposes the slowly varying ramp in the y^+ electrode is either replaced by a DC signal or assumed to be earthed or open circuited, (G. Schitter and A. Stemmer, 2004; N. Tamer and M. Daleh, 1994).

In Figure 8 the capacitive sensor response C_x , to a triangular waveform input of amplitude $3.3\mu\text{coulombs}$ and fundamental frequency of 40Hz at the x^+ electrode with the y^+ electrode being earthed is plotted. Note that the capacitive sensor output C_x is not exactly a triangular waveform, but appears to be equal to a triangular waveform plus certain periodic corrugations. The distortion in the capacitive sensor output C_x is due to the amplification of the 21st and the 23rd harmonics of the triangular waveform which are close to the resonance frequency of the piezoelectric tube. A

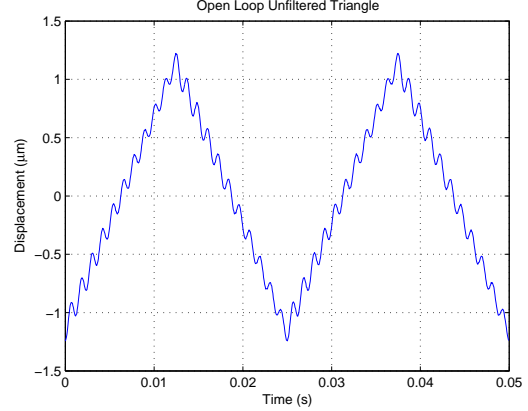


Fig. 8. Response recorded by the capacitive sensor C_x for a triangular waveform input with amplitude $3.3\mu\text{ coulombs}$ and fundamental frequency 40Hz.

standard practice to eliminate the periodic corrugations at the output C_x , is to use a feedback controller and damp the resonant mode which causes the amplification.

4. POSITIVE VELOCITY AND POSITION FEEDBACK CONTROLLER

In this section, the concept of Positive Velocity and Position Feedback (PVPF) control is introduced, and a design procedure, linking the output

V_{x-} to the input Q_{x+} , is presented to damp the resonant mode using a PVPF controller.

In the current context, Positive Velocity and Position Feedback (PVPF) controller is defined by the second order controller

$$K_{PVPF}(s) \triangleq \frac{\Gamma_1 s + \Gamma_2}{s^2 + 2\xi w s + w^2}, \quad (7)$$

where ξ, w, Γ_1 and Γ_2 are the design parameters.

Since the feedback is positive, it can be checked that the transfer-function relating the reference signal $r(t)$, which is the triangular waveform, inputted at x^+ and the output x^- is given by

$$G_{xx}^{cl}(s) = \frac{G_{xx}(s)}{1 - G_{xx}(s)K_{PVPF}(s)}. \quad (8)$$

It can be checked from (8) that the poles of the closed-loop system are the roots of the polynomial

$$\begin{aligned} P(s) = & s^4 + (2\sigma\omega + (2\xi w - \Gamma_1 d))s^3 \\ & + (\omega^2 + 2\sigma\omega(2\xi w - \Gamma_1 d) + (w^2 - \Gamma_2 d))s^2 \\ & + (2\sigma\omega(w^2 - \Gamma_2 d) + (2\xi w - \Gamma_1 d)\omega^2 - k_1\Gamma_1)s \\ & + \omega^2(w^2 - \Gamma_2 d) - k_1\Gamma_2. \end{aligned} \quad (9)$$

For the closed loop system to be well damped, it is desirable to have the roots of polynomial $P(s)$ well inside the left half plane. Assume that $\{p_i\}_{i=1}^4$ are the desired pole positions of the closed loop system and

$$Q(s) \triangleq s^4 + K_1 s^3 + K_2 s^2 + K_3 s + K_4 \quad (10)$$

is the corresponding polynomial with roots $\{p_i\}_{i=1}^4$. Matching the coefficients of $P(s)$ and $Q(s)$ would give

$$2\sigma\omega + 2\xi w - \Gamma_1 d = K_1 \quad (11)$$

$$\omega^2 + 2\sigma\omega(2\xi w - \Gamma_1 d) + (w^2 - \Gamma_2 d) = K_2 \quad (12)$$

$$2\sigma\omega(w^2 - \Gamma_2 d) + (2\xi w - \Gamma_1 d)\omega^2 - \Psi\Gamma_1 = K_3 \quad (13)$$

and

$$\omega^2(w^2 - \Gamma_2 d) - \Psi\Gamma_2 = K_4. \quad (14)$$

Note that the equations (11)-(14) are linear in $2\xi w, w^2, \Gamma_1$ and Γ_2 , and can be solved for them to get the PVPF controller $K_{PVPF}(s)$. However, for the controller $K_{PVPF}(s)$ to be stable, or even meaningful, the quantities $2\xi w$ and w^2 , have to be positive. Therefore the desired polynomial coefficients K_1, K_2, K_3 and K_4 have to be such that equations (11)-(14) yield positive solutions for $2\xi w$ and w^2 .

5. NUMERICAL ILLUSTRATIONS AND EXPERIMENTS USING THE PVPF CONTROLLER

In this section, first a PVPF controller connecting the output V_{x-} to the input Q_{x+} is constructed to

damp the resonant mode of the piezoelectric tube, and the closed loop system is then actuated in a raster pattern.

Note that poles of $G_{xx}(s)$, computed from (5), are

$$p_{\pm} = -39.5 \pm i5424.4. \quad (15)$$

Here the desired closed-loop poles are set to

$$P_{1+} = P_{2+} = -2039.5 \pm i5424.4, \quad (16)$$

$$P_{1-} = P_{2-} = -2039.5 \pm i5424.4.$$

which amounts to placing the closed-loop poles of the system further into the left half plane by 2000 units. It can be checked that the polynomial coefficients corresponding to the desired poles (16) are $K_1 = 8.158 \times 10^3$, $K_2 = 8.381 \times 10^7$, $K_3 = 2.74 \times 10^{11}$ and $K_4 = 1.128 \times 10^{15}$. Solving for the controller parameters Γ_1, Γ_2, ξ and w from equations (11)-(14), gives the PVPF controller

$$K_{PVPF}(s) \triangleq \frac{-6564s + 9.302 \cdot 10^7}{s^2 + 8591s + 4.649 \cdot 10^7}. \quad (17)$$

In order to actuate the closed-loop system in a raster pattern, a triangular waveform of amplitude 3.3μ coulombs and fundamental frequency 40Hz is inputted at the x^+ electrode with the y^+ electrode being earthed. The response C_x recorded by the capacitive sensor to that input is plotted in Figure 9. It is apparent that the periodic cor-

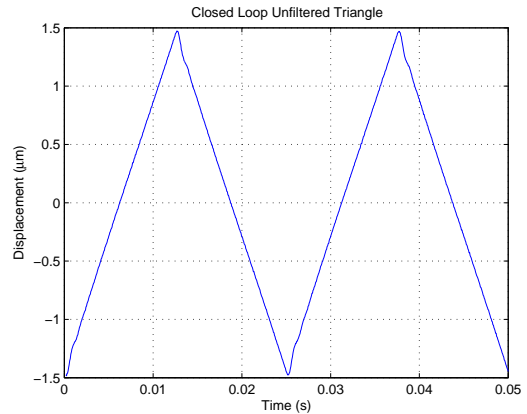


Fig. 9. Response recorded by the capacitive sensor C_x for a triangular waveform input of 3.3μ coulombs and 40Hz.

ruptions in open-loop capacitive sensor response C_x are not present in the closed-loop response. In Figure 10 the closed-loop frequency responses (FRFs) $G_{xc_x}^{(cl)}(i\omega)$ and $G_{xc_y}^{(cl)}(i\omega)$ relating the input x^+ and the outputs at C_x and C_y respectively are plotted. Note that, the resonance mode of the closed loop FRF $G_{xc_x}^{(cl)}(i\omega)$ is damped by about

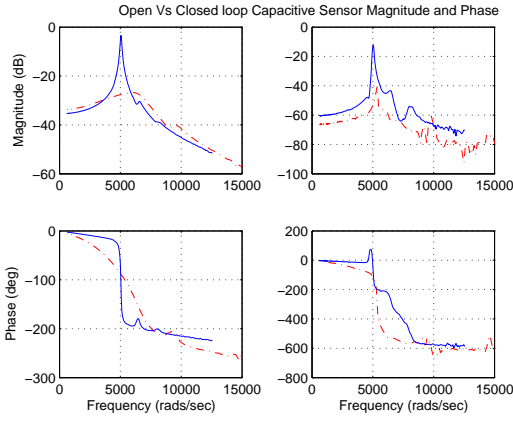


Fig. 10. Closed loop magnitude response of the subsystem C (dashed dots) along with its open loop counterpart (solid).

30dB when compared with the open loop FRF $G_{xc_x}(i\omega)$. Hence, as a consequence the harmonics of the triangular waveform close to the resonance are not amplified.

However, the response plotted in Figure 9 is not really a smooth triangular waveform, in particular near the peaks of the response. In order to rectify this problem, instead of using a triangular waveform as input, the input signal is shaped such that the corresponding output at C_x is the desired triangular waveform. In other words instead of using a triangular waveform as input, the following signal is used as the input:

$$u(t) \triangleq \sum_{k=1}^{\infty} \frac{a_k}{|G_{xc_x}^{(cl)}(i\omega_k)|} \sin(\omega_k t - \phi_k), \quad (18)$$

where a_k and ω_k are the Fourier components of the desired triangular waveform, $G_{xc_x}^{(cl)}(i\omega)$ denotes the FRF obtained by fitting a parametric model to the non-parametric data plotted in Figure 10 and $\phi_k = \angle G_{xc_x}^{(cl)}(i\omega_k)$. The response at C_x to the input $u(t)$, (18), is plotted in Figure 11. Note that it is a smooth triangular waveform.

6. CONCLUSIONS

A piezoelectric tube of the type typically used in STMs and AFMs is considered for actuation. Actuation of this tube is hampered by presence of resonant modes and hysteresis. Hysteresis, generally observed while actuating piezoelectric materials, is negated by actuating the tube using charge sources, as opposed to using voltage sources. The piezoelectric tube is modeled as a linear system, and a lightly damped resonant mode hampering the actuation of the tube is identified. The concept of PVPF control is introduced, and a design procedure to damp the resonant mode using a PVPF controller is presented. It is observed that using a

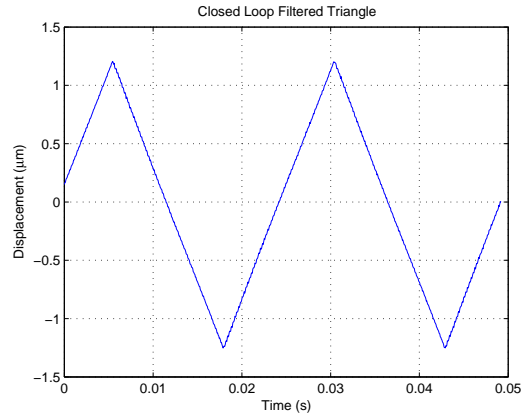


Fig. 11. Response recorded by the capacitive sensor C_x for an input of the form (18) with amplitude $3.3\mu\text{coulombs}$ and fundamental frequency 40Hz.

PVPF controller a 30dB damping of the resonant mode can be achieved without much control effort. Inputs are shaped based on the closed loop system to accurately actuate the piezoelectric tube in a raster pattern.

REFERENCES

- A. J. Fleming and S. O. R. Moheimani (Feb 2003). Precision Current and Charge Amplifiers for Driving High Capacitive Piezoelectric Loads.. *Electronic Letters* **39**(3), 282–284.
- G. Schitter and A. Stemmer (2004). Identification and Open-Loop Tracking Control of a Piezoelectric Tube Scanner for High-Speed Scanning Probe Microscopy. *IEEE Transactions on Control Systems Technology* **12**(3), 449–454.
- Ge, P. and M. Jouaneh (1996). Tracking control of a piezoelectric actuator. *IEEE Transactions on control systems technology* **4**(3), 209–216.
- J. L. Fanson and T. K. Caughey (1990). Positive Position Feedback Control for Large Space Structures. *AIAA Journal* **28**(4), 717–724.
- K. K. Leang and S. Devasia (2002). Hysteresis, Creep and Vibration Compensation for Piezoactuators: Feedback and Feedforward Control. *Proc. of 2nd IFAC Conference on Mechatronic Systems Berkeley, California, USA* pp. 283–289.
- N. Tamer and M. Dahleh (1994). Feedback Control of Piezoelectric Tube Scanners. *in Proc. of the 33rd Conference on Decision and Control, Lake Buena Vista, Florida* pp. 1826–1831.
- Newcomb, C. V. and I. Flinn (1982). Improving the linearity of piezoelectric ceramic actuators. *IEE Electronics Letters* **18**(11), 442–443.